Geopersia 2022, 12(1): 53-68
DOI: 10.22059/GEOPE.2021.321412.648607

RESEARCH PAPER

# Analytical hierarchical prospectivity mapping using integration of exploratory data in the Anarak region, Central Iran

**Somayeh Panahi [1], Ahmad Khakzad [1], Peyman Afzal [2,*]**

[1] Department of Geology, North Tehran Branch, Islamic Azad University, Tehran, Iran
[2] Department of Petroleum and Mining Engineering, South Tehran Branch, Islamic Azad University, Tehran, Iran

Received: 03 April 2021, Revised: 29 June 2021, Accepted: 26 July 2021


**Abstract**
This paper aims to show the kind of corporations, Analytical Hierachy Process (AHP) for determining significant weights of evaluation criteria with "Technique for Order Preference by Similarity to Ideal" (TOPSIS) and "Simple Additive Weighting" (SAW) methods for ranking of geo-dataset for Mineral Prospectivity Mapping (MPM) of Cu in Anarak region, Central Iran. This operation was carried out by integration of remote sensing, geophysical, geochemical and geological data. The Anarak region has a high potential for copper mineralization because the studied district is located in the NW of the Central East Iranian Microplate (CEIM) that is an important ore mineralized zone in Central Iran. The integration approaches are complex, Multi-Criteria Decision Making (MCDM), and knowledge-driven methods that they named AHP-TOPSIS and AHP-SAW. In addition, there are three variant models of TOPSIS method including conventional, adjusted and modified. The AHP has been carried out on geological/alteration data, structural data, airborne geophysical data and stream sediment geochemical layer in the studied area. These data are classified by fractal modeling for the generation of geo-dataset layers to a relationship of copper occurrences in the Anarak region. Consequently, the produced MPMs by the AHP-TOPSIS and AHP-SAW have adequately matching and sufficient correlation with copper mines and main copper deposits/occurrences in the Anarak region.

**Keywords:** AHP-TOPSIS; AHP-SAW; Copper; Anarak.

## Introduction

Multi-Criteria Decision Making (MCDM) methods have been outspreading applications in recent decades and used in various research branches, for instance, obtaining ore potential locations in mineral exploration. The decision-maker purposes to solve the MCDM problems with optimal solutions. Generally, the MCDM methods used to geo-datasets such as geochemical, geological, geophysical, and remote sensing data for regional exploration due to Mineral Prospectivity Mapping (MPM) by Geographical Information System (GIS). The MCDM techniques contain two distinct types: the data-driven and knowledge-driven (Saaty & Vargas, 2001; Zhang et al., 2017; Panahi et al., 2017, Ferrier et al., 2019; Ghaeminejad et al., 2020).

The study suggests that the MCDM methods have a varied range such as Preference Ranking Organization Method for Enrichment Evaluation Simple Additive Weighting (SAW) (Churchman & Ackoff, 1954), Analytic Hierarchy Process (AHP) (Saaty & Vargas, 2001), Vise Kriterijumska Optimizacija I Kompromisno Resenje (VIKOR) ( Opricovic & Tzeng, 2004), Elimination and choice Expressing Reality (ELECTRE) ( Almeida-Dias et al., 2010) and

* Corresponding author e-mail: p_afzal@azad.ac.ir

Weighted Aggregates Sum Product Assessment (WASPAS) (Zavadskas et al., 2012).

The AHP is used for Order Preference by Similarity to Ideal Solution (TOPSIS) which was presented by Hwang and Yoon (1981). The AHP is utilized to calculate the weight of multiple criteria including geological, geophysical, and geochemical data. The TOPSIS chooses the best selection of alternatives, based on the minimum distance from the Positive Ideal Solution (PIS) and maximizes distance from Negative Ideal Solution (NIS).

In this study, the TOPSIS and SAW in combination with the AHP are presented for obtaining the copper MPM by nine exploratories as criteria and subsequently in the Anarak region (central Iran; Fig. 1). The validation of the AHP-TOPSIS and AHP-SAW were calculated by matching of correlation between the location of Cu mines and the high potential of MPM.

## Geological setting

The Anarak is located 220 km northeast of Isfahan and 76 km northeast of Nain city. This region is located on the southern edge of the desert plain (Central desert; Fig. 1). This area is a significant mineralized zone that is known as the Anarak Metamorphic Complex (AMC) (Buchs et al., 2013) by two major mineralization phases: copper volcanogenic mineralization and superprinted ores such as an association of Cu, Ni, Co, and U ores (Tarkian et al., 1983). The AMC subdivide into three domains including Carboniferous, Permo-Teriassic, and Teriassic (Bagheri et al., 2007). The main reason for the well-known deposits is hosted by Magmatic rocks at the intersection of the active Great Kavir-Druneh fault by the length of 700 km and the Uremia-Dokhtar Magmatic Belt (UDMB) (Bagheri, 2015).

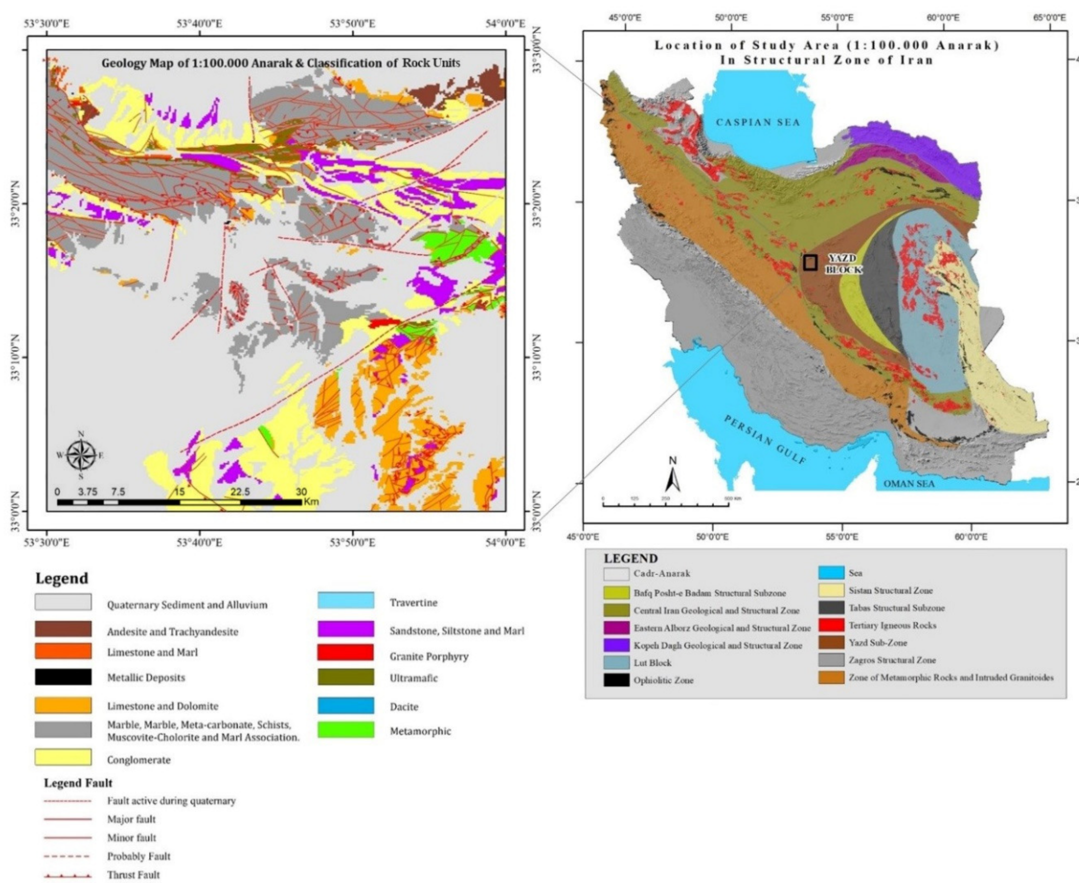


**Figure 1.** Location of the studied area in the generalized 1:100000 scale geological map in Isfahan province of Iran (Sahandi et al., 2005)

Furthermore, there are some metamorphic rocks because crustal-scale lineaments are deep-seated and extremely active during mineralization in the genesis of the mineral deposits in this region (Bagheri, 2015). Some vein and manto type deposits have been explored for Cu, Ni, Co, and U in the Anarak region (Jebeli et al., 2020). Two main mineralization phases are recognized: the first phase comprises copper volcanogenic mineralization in the Eocene age and the second mineralization phase includes accumulation of the Cu, Ni, Co, and U ores which are superprinted ores (Tarkian et al., 1983). These ore deposits are hosted by magmatic and metamorphic rocks.

A 1:100,000 geological map of Anarak contains rock units' information, faults, and Cu occurrences. Moreover, the geochemical data is collected from samples of stream sediment for generation of a geochemical map. There are 678 stream sediment samples which are analyzed for 35 elements by the ICP-MS method. Airborne magnetic surveys used for the geophysical datasets and alteration zones are delineated by remote sensing datasets. The survey of Anarak is regional and covers 1353 magnetic points within 7.5-km profiles.

## Methodology

### *AHP*

The AHP method along with GIS techniques plays a very beneficial role in various fields (Maity & Mandal, 2019). This method is a set of pairwise comparisons from the estimation of appropriate data. The AHP contains three steps for defining the weight of the criteria which are as follows (Zhang et al., 2017):

1) The complex decision structure is essential to the process of the AHP that it comprises on aim at the top, multi-criteria and sub-criteria in the middle, and decision alternatives at the bottom, as depicted in Fig. 3.

2) Organizing pairwise comparisons according to a standardized comparison scale of nine ranks in Table 1, according to the relative significance of the different criteria. Let C = {$C_j$| j=1, 2, 3, …, n} be the set of criteria. Matrix A indicates ratios of weights with $a_{ij}$ for every criterion and the diagonal elements of the matrix are 1, as follows:

$$A=\begin{bmatrix} a_{11} & \cdots & a_{1n} \\ \vdots & \ddots & \vdots \\ a_{n1} & \cdots & a_{nn} \end{bmatrix}, \quad a_{ii=1}, \quad a_{ji=} 1/a_{ij}, \quad a_{ij\neq} 0. \tag{1}$$

3) The mathematical procedure has to be normalized and calculate the relative weights for every matrix. $\lambda_{max}$ is the largest eigenvalue of the A and w that they can be determined by the equation:

$$A\times w = \lambda_{max} \times w \tag{2}$$

**Table 1.** Nine-point intensity of importance scale and its description (Saaty & Vargas, 2001).

| Intensity of importance | Definition |
|---|---|
| 1 | Equal importance or preference |
| 2 | Equal to moderate importance or preference |
| 3 | Moderate importance or preference |
| 4 | Moderate to strong importance or preference |
| 5 | Strong importance or preference |
| 6 | Strong to very strong importance or preference |
| 7 | Very strong importance or preference |
| 8 | Very to extremely strong importance or preference |
| 9 | Extreme importance or preference |

The consistency index has strictly related to the quality of the output. The consistency is distinct by the relation among the entries of A: $a_{ij} \times a_{jk} = a_{ik}$. The consistency index, CI is intended as:

CI = ($\lambda_{max}$-n)/(n-1) (3)

At the last, the consistency ratio (CR) is calculated as the CI and the random index (RI) as assumed in Equation 8 (Ying et al. 2007), The CR has to less than 0.1.

CR = CI/RI, CR< 0.1 (4)

*TOPSIS*

The principal concept of the TOPSIS is that the best chosen alternative should be the nearest distance from the PIS and the farthest distance from the NIS (Fig 2) (Opricovic & Tzeng, 2004; Pazand & Hezerkhani, 2015). There are three types of TOPSIS that they were Conventional TOPSIS (C-TOPSIS) (Hwang & Yoon, 1981), Adjusted TOPSIS (A-TOPSIS) (Deng et al., 2000), and Modified TOPSIS (M-TOPSIS) (Rent et al., 2007).

*C-TOPSIS method*

The n and m show alternatives and criteria by number series of $A_i$ $(i = 1, 2, \ldots, n)$ and $C_j$ $(j = 1, 2, \ldots, m)$. The eight formulation steps of the TOPSIS are as follows:

1) It should be noted that the decision matrix is based on every MCDM procedure. The structure of that consist of $A_i$ $(i = 1, 2, \ldots, n)$ and $C_j (j = 1, 2, \ldots, m)$. Moreover, i and j denote the alternative and criteria, respectively. Specifically, this matrix allocates a priority score $X = (x_{ij})_{n \times m}$ to every i on each j.

2) The total weight ($w_j$) of the criteria is calculated by the following equation:

$$\sum_{i=1}^{m} w_j = 1, j = 1, 2, \ldots, m.. \quad (5)$$

3) Determine the normalized decision matrix ($r_{ij}$) for every column. This step can remove scaling effects problems of the TOPSIS method.

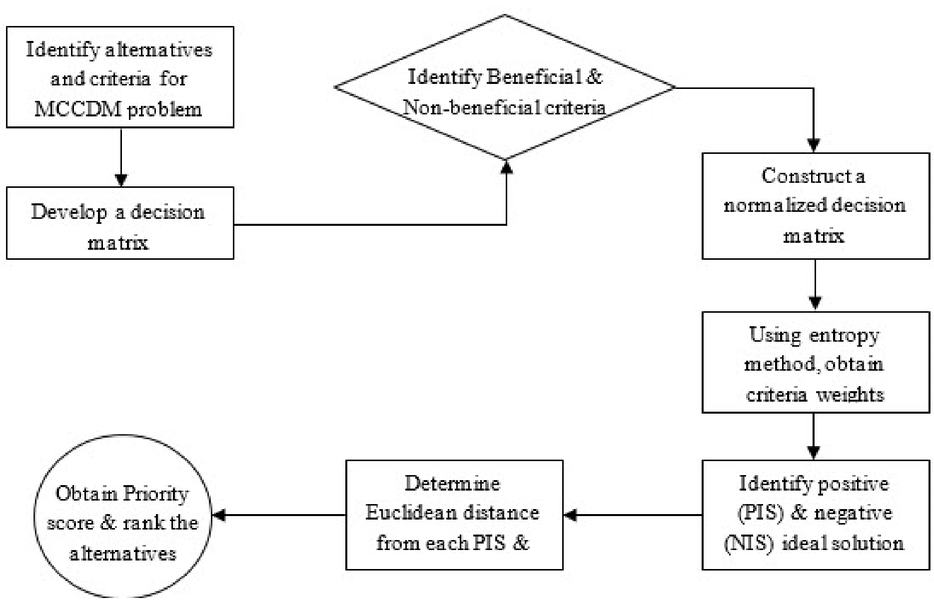


**Figure 2.** The proposed flowchart of TOPSIS method

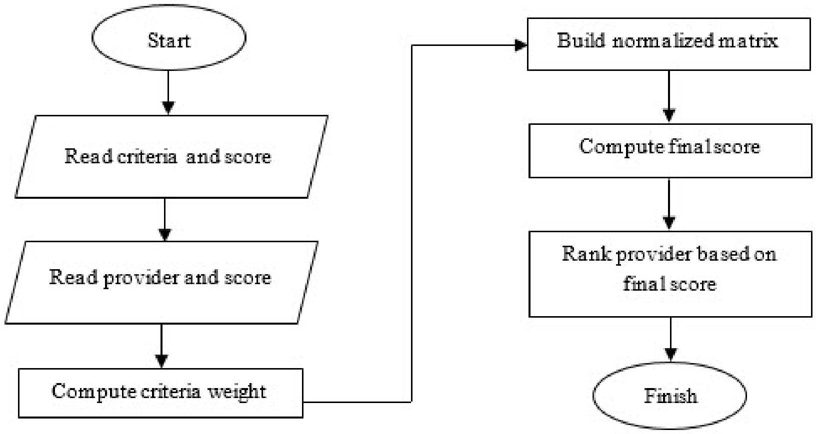


**Figure 3.** The flowchart of SAW method

$$r_{ij} = \frac{x_{ij}}{\sqrt{\sum_{p=1}^{n} x_{pj}^2}}, i = 1, 2, \dots, n; j = 1, 2, \dots, m \quad (6)$$

4) Compute the weighted normalized decision matrix of $V_{ij}$,

$$V_{ij} = w_j r_{ij}, i = 1, 2, .., n; j = 1, 2, \dots, m \quad (7)$$

5) Find the PIS and NIS values, respectively, there are:

$$f^+ = (v_1^+, v_2^+, \dots, v_j^+, \dots, v_m^+) = \left\{ (\max_i \{v_{ij}\} | j \in B), (\min_i \{v_{ij}\} | j \in C) \right\} \quad (8)$$

$$f^- = (v_1^-, v_2^-, \dots, v_j^-, \dots, v_m^-) = \left\{ (\min_i \{v_{ij}\} | j \in B), (\max_i \{v_{ij}\} | j \in C) \right\} \quad (9)$$

6) There follows the separation measures M= $(S_i^+, S_i^-)$ are calculated by Euclidean distance.

$$S_i^+ = \sqrt{\sum_{j=1}^{m} (v_{ij} - v_j^+)^2} \quad ; i = 1, \dots, n \quad (10)$$

$$S_i^- = \sqrt{\sum_{j=1}^{m} (v_{ij} - v_j^-)^2} \quad ; i = 1, \dots, n \quad (11)$$

7) Compute the relative closeness of the alternatives to the ideal solution as follows:

$$T_i^C = \frac{S_i^-}{S_i^+ + S_i^-} \; ; i = 1, \dots, n \quad (12)$$

8) Determine the normalized the MPM values of $M_i^C$ for final prospectivity mapping as:

$$M_i^C = \frac{T_i^C - \min_i (T_i^C)}{\max_i (T_i^C) - \min_i (T_i^C)} ; i = 1, \dots, n; 0 \le M_i^C \le 1 \quad (13)$$

High and low potential zones correlate with high and low values of $M_i^C$ in studied area.

*A-TOPSIS method*

The A-TOPSIS that the weighted Euclidian distances put instead of the weighted decision

matrix of $V_{ij}$ by eight equations:
1-3) Similar to the steps of C-TOPSIS method, including a priority score $X = (x_{ij})_{n\times m}$, weight of all criteria ($w_j$), and normalized decision matrix ($r_{ij}$).

4) Compute the PIS and NIS values, respectively, as:
$$f^+ = (v_1^+, v_2^+, \dots, v_j^+, \dots, v_m^+) = \{(\max_i \{r_{ij}\} | j \in B), (\min_i \{r_{ij}\} | j \in C)\} \quad (14)$$
$$f^- = (v_1^-, v_2^-, \dots, v_j^-, \dots, v_m^-) = \{(\min_i \{r_{ij}\} | j \in B), (\max_i \{r_{ij}\} | j \in C)\} \quad (15)$$

5) Calculate the weighted Euclidian distances,
$$S_i^+ = \sqrt{\sum_{j=1}^{m} w_j (r_{ij} - v_j^+)^2} \quad ; i = 1, \dots, n \quad (16)$$
$$S_i^- = \sqrt{\sum_{j=1}^{m} w_j (r_{ij} - v_j^-)^2} \quad ; i = 1, \dots, n \quad (17)$$

6) Obtain the relative closeness of the alternatives to the ideal solution as follows:
$$T_i^A = \frac{S_i^-}{S_i^+ + S_i^-} \ ; i = 1, \dots, n \quad (18)$$

7) Calculate the normalized MPM values of $M_i^A$ for final prospectivity mapping as:
$$M_i^A = \frac{T_i^A - \min_i (T_i^A)}{\max_i (T_i^A) - \min_i (T_i^A)} \quad ; i = 1, \dots, n; 0 \le M_i^A \le 1 \quad (19)$$

M-TOPSIS method

1-5) Similar to the step of C-TOPSIS method.
6) Obtain the ideal reference point S as:
$$S = (S^l, S^N) = (\min (S_i^+), \max(S_i^-)) \ ; i = 1, \dots, n \quad (20)$$

7) Determine Euclidian distance between the point S and the values of $S_i^+$ *and* $S_i^-$ for every sub-criteria, that is:
$$T_i^M = \sqrt{(S_i^+ - S^l)^2 + (S_i^- - S^N)^2} \quad ; i = 1, \dots, n \quad (21)$$

8) Calculate the normalized MPM values of $M_i^M$ for final prospectivity mapping, as:
$$M_i^M = \frac{\max_i (T_i^M) - T_i^M}{\max_i (T_i^M) - \min_i (T_i^M)} \quad ; i = 1, \dots, n; 0 \le M_i^M \le 1 \quad (22)$$

*SAW*

The SAW method is a kind of Multiple Attribute Decision-making (MADM) technique (Fig. 3). There are two steps in this method.

1) Obtain normalized values of the decision matrix elements as follows:
$$r_{ij} = \frac{d_{ij}}{d_j^{max}}, \qquad d_j^{max} = \max d_{ij} \quad ; 1 \le i \le m; j = 1, 2, \dots, k; \quad \text{for profit attributes} \quad (23)$$

$$r_{ij}=\frac{d_j^{min}}{d_{ij}}, \qquad d_j^{min}=\min d_{ij} \quad ;1\leq i\leq m; j=1,2,\dots,k; \qquad \text{for cost attributes} \qquad (24)$$

2) Calculate final score of each alternative as:

$$P_i=\sum_{j=1}^{k} w_j.r_{ij}, i=1,2,\dots,m. \qquad (25)$$

## Calculate the weight of Sub-Criteria

*Sub-Criteria weighting by AHP*

The AHP process is determining weights of data by expert's subjective judgment:
1) Define pairwise comparison information for an integrated matrix according to the definition scales (Table 1). The pairwise comparison matrix uses criteria including geological, geophysical, and geochemical data. These consist of sub-criteria as surface data (rock-fault), remote sensing (alteration zones), airborne magnetic and stream sediment data.
2) Compute the final criteria weights by Eq. (2) as depicted in Table 2.

*Design concept priority ranking by AHP-TOPSIS*

The obtained results of AHP can't be precise (Zhu et al., 2020); therefore, AHP is rated by TOPSIS to achieve accurate and realistic results. The steps AHP-Conventional-TOPSIS (ACT) are following forms:
1) The decision matrix of TOPSIS was constructed by alternatives and nine criteria of Anarak datasets according to nine criteria intensity of AHP (Table 1), this decision matrix is based on the collection of experts' interviews (Table 3).
2) Use AHP in this step of TOPSIS for the weight of criteria similar to Eq. (5) as shown in Table 2.
3) Calculate the normalized decision matrix by Eq. (6; Table 4).
4) Construct the weighted normalized decision matrix based on Eq. (7) as depicted in Table 5.
5) Find PIS and NIS for CC-TOPSIS by Eqs. (8-9; Table 6).
6) Calculate the separation measures based on Eqs. (10- 11).
7) The relative closeness of the alternatives to the ideal solution by Eq. (12).
8) The normalized MPM data values of $M_i^C$ are computed by Eq. (13; Table 8).

**Table 2.** Results of the AHP method in weighting for the assessed criteria, sub-criterion and alternatives

| Data | Weight | Criterion | weight | Sub-criteria | Weight | Final weight |
|---|---|---|---|---|---|---|
| **Geological data** | 0.525 | Surface study | 0.667 | Rock | 0.750 | 0.263 |
| | | | | Fault | 0.250 | 0.088 |
| | | Remote sensing | 0.333 | Argilic | 0.409 | 0.071 |
| | | | | Phyllic | 0.256 | 0.045 |
| | | | | Feoxides | 0.186 | 0.033 |
| | | | | Silicic | 0.091 | 0.016 |
| | | | | Prophylitic | 0.059 | 0.010 |
| **Geophysical data** | 0.142 | Airborne magnetic | 1.00 | Analytical signal | 1.000 | 0.142 |
| **Geochemical data** | 0.334 | Stream sediment sample | 1.00 | cu | 1.000 | 0.334 |

**Table 3.** The pairwise comparison matrices are built Based on the knowledge and judgment of experts for alternatives according to Table1

| Alternatives | | | Sub-criteria | | | | | | | | |
|---|---|---|---|---|---|---|---|---|---|---|---|
| **Num** | **x(m)** | **y(m)** | **Rock** | **Fault** | **Arg.** | **Phy.** | **Feo.** | **Si.** | **Pro.** | **As.** | **Cu** |
| **1** | 535800 | 331400 | 1 | 6 | 1 | 1 | 1 | 1 | 5 | 1 | 1 |
| **2** | 533500 | 332000 | 9 | 5 | 7 | 2 | 1 | 1 | 6 | 5 | 7 |
| **3** | 533830 | 332200 | 9 | 5 | 1 | 1 | 1 | 1 | 4 | 5 | 7 |
| **4** | 533100 | 332300 | 9 | 5 | 4 | 1 | 6 | 2 | 4 | 4 | 9 |
| **5** | 533600 | 332300 | 9 | 7 | 7 | 5 | 5 | 6 | 8 | 7 | 7 |
| **6** | 534100 | 332300 | 1 | 5 | 1 | 1 | 1 | 3 | 5 | 6 | 3 |
| **7** | 533000 | 332300 | 1 | 3 | 4 | 1 | 4 | 1 | 1 | 3 | 9 |
| **8** | 533200 | 332300 | 9 | 6 | 4 | 6 | 4 | 8 | 9 | 3 | 7 |
| **9** | 533300 | 332300 | 9 | 8 | 3 | 6 | 3 | 4 | 8 | 3 | 6 |
| **10** | 533900 | 332300 | 9 | 5 | 1 | 1 | 1 | 1 | 2 | 4 | 6 |
| **11** | 533300 | 332400 | 1 | 7 | 3 | 6 | 3 | 9 | 7 | 3 | 3 |
| **12** | 533400 | 332400 | 9 | 7 | 1 | 1 | 6 | 3 | 8 | 2 | 3 |
| **13** | 533500 | 332400 | 1 | 5 | 3 | 1 | 9 | 4 | 6 | 2 | 3 |
| **14** | 533630 | 332400 | 1 | 5 | 2 | 5 | 6 | 1 | 5 | 2 | 3 |
| **15** | 533700 | 332400 | 1 | 3 | 1 | 5 | 3 | 1 | 6 | 2 | 1 |
| **16** | 534000 | 332400 | 1 | 5 | 1 | 1 | 1 | 1 | 1 | 3 | 5 |
| **17** | 534300 | 332400 | 1 | 5 | 1 | 1 | 1 | 2 | 5 | 3 | 1 |
| **18** | 533200 | 332500 | 9 | 7 | 1 | 2 | 2 | 8 | 9 | 1 | 5 |
| **19** | 533630 | 332500 | 1 | 3 | 1 | 1 | 2 | 1 | 2 | 1 | 3 |
| **20** | 534700 | 332500 | 1 | 8 | 1 | 1 | 1 | 1 | 4 | 1 | 4 |
| **21** | 534900 | 332500 | 9 | 7 | 1 | 1 | 3 | 2 | 7 | 1 | 7 |
| **22** | 533200 | 332600 | 1 | 5 | 7 | 1 | 2 | 4 | 7 | 1 | 3 |
| **23** | 535800 | 332700 | 1 | 2 | 1 | 1 | 1 | 1 | 1 | 1 | 3 |
| **24** | 535900 | 332700 | 9 | 2 | 1 | 1 | 1 | 1 | 1 | 1 | 3 |

**Table 4.** The normalized decision matrix in TOPSIS method

| Alternatives | | | Sub-criteria | | | | | | | | |
|---|---|---|---|---|---|---|---|---|---|---|---|
| **Num** | **x(m)** | **y(m)** | **Rock** | **Fault** | **Arg.** | **Phy.** | **Feo.** | **Si.** | **Pro.** | **As.** | **Cu** |
| **1** | 535800 | 331400 | 0.031 | 0.222 | 0.064 | 0.068 | 0.056 | 0.053 | 0.178 | 0.062 | 0.039 |
| **2** | 533500 | 332000 | 0.280 | 0.185 | 0.446 | 0.136 | 0.056 | 0.053 | 0.213 | 0.311 | 0.270 |
| **3** | 533830 | 332200 | 0.280 | 0.185 | 0.064 | 0.068 | 0.056 | 0.053 | 0.142 | 0.311 | 0.270 |
| **4** | 533100 | 332300 | 0.280 | 0.185 | 0.255 | 0.068 | 0.338 | 0.105 | 0.142 | 0.249 | 0.347 |
| **5** | 533600 | 332300 | 0.280 | 0.259 | 0.446 | 0.341 | 0.282 | 0.315 | 0.284 | 0.249 | 0.193 |
| **6** | 534100 | 332300 | 0.155 | 0.185 | 0.064 | 0.068 | 0.056 | 0.158 | 0.178 | 0.374 | 0.116 |
| **7** | 533000 | 332300 | 0.280 | 0.111 | 0.255 | 0.068 | 0.225 | 0.053 | 0.063 | 0.187 | 0.347 |
| **8** | 533200 | 332300 | 0.280 | 0.222 | 0.255 | 0.409 | 0.225 | 0.420 | 0.320 | 0.187 | 0.270 |
| **9** | 533300 | 332300 | 0.280 | 0.296 | 0.191 | 0.409 | 0.169 | 0.210 | 0.284 | 0.187 | 0.231 |
| **10** | 533900 | 332300 | 0.155 | 0.185 | 0.064 | 0.068 | 0.113 | 0.053 | 0.036 | 0.311 | 0.270 |
| **11** | 533300 | 332400 | 0.280 | 0.259 | 0.191 | 0.409 | 0.169 | 0.473 | 0.249 | 0.249 | 0.193 |
| **12** | 533400 | 332400 | 0.280 | 0.259 | 0.064 | 0.136 | 0.338 | 0.210 | ٠,٣٢٠ | 0.187 | 0.231 |
| **13** | 533500 | 332400 | 0.031 | 0.185 | 0.191 | 0.068 | 0.507 | 0.210 | 0.213 | 0.125 | 0.116 |
| **14** | 533630 | 332400 | 0.031 | 0.185 | 0.128 | 0.341 | 0.338 | 0.053 | 0.178 | 0.125 | 0.116 |
| **15** | 533700 | 332400 | 0.031 | 0.111 | 0.064 | 0.341 | 0.169 | 0.053 | 0.213 | 0.125 | 0.039 |
| **16** | 534000 | 332400 | 0.062 | 0.185 | 0.128 | 0.068 | 0.113 | 0.105 | 0.107 | 0.249 | 0.193 |
| **17** | 534300 | 332400 | 0.031 | 0.185 | 0.064 | 0.068 | 0.056 | 0.105 | 0.178 | 0.187 | 0.039 |
| **18** | 533200 | 332500 | 0.280 | 0.259 | 0.128 | 0.205 | 0.169 | 0.473 | 0.320 | 0.249 | 0.231 |
| **19** | 533630 | 332500 | 0.031 | 0.111 | 0.064 | 0.068 | 0.113 | 0.053 | 0.071 | 0.062 | 0.116 |

| | | | | | | | | | | | |
|---|---|---|---|---|---|---|---|---|---|---|---|
| **20** | 534700 | 332500 | 0.031 | 0.296 | 0.064 | 0.068 | 0.056 | 0.053 | 0.142 | 0.062 | 0.154 |
| **21** | 534900 | 332500 | 0.280 | 0.259 | 0.064 | 0.068 | 0.169 | 0.105 | 0.249 | 0.062 | 0.270 |
| **22** | 533200 | 332600 | 0.031 | 0.185 | 0.446 | 0.068 | 0.113 | 0.210 | 0.249 | 0.062 | 0.116 |
| **23** | 535800 | 332700 | 0.031 | 0.074 | 0.064 | 0.068 | 0.056 | 0.053 | 0.036 | 0.062 | 0.116 |
| **24** | 535900 | 332700 | 0.280 | 0.074 | 0.064 | 0.068 | 0.056 | 0.053 | 0.036 | 0.125 | 0.116 |

**Table 5.** The weighted normalized decision matrix in TOPSIS method

| **Alternatives** | | | **Sub-criteria** | | | | | | | | |
|---|---|---|---|---|---|---|---|---|---|---|---|
| **Num** | **x(m)** | **y(m)** | **Rock** | **Fault** | **Arg.** | **Phy.** | **Feo.** | **Si.** | **Pro.** | **As.** | **Cu** |
| **1** | 535800 | 331400 | 0.008 | 0.020 | 0.005 | 0.003 | 0.002 | 0.001 | 0.002 | 0.009 | 0.013 |
| **2** | 533500 | 332000 | 0.074 | 0.016 | 0.032 | 0.006 | 0.002 | 0.001 | 0.002 | 0.044 | 0.090 |
| **3** | 533830 | 332200 | 0.074 | 0.016 | 0.005 | 0.003 | 0.002 | 0.001 | 0.001 | 0.044 | 0.090 |
| **4** | 533100 | 332300 | 0.074 | 0.016 | 0.018 | 0.003 | 0.011 | 0.002 | 0.001 | 0.035 | 0.116 |
| **5** | 533600 | 332300 | 0.074 | 0.023 | 0.032 | 0.05 | 0.009 | 0.005 | 0.003 | 0.035 | 0.064 |
| **6** | 534100 | 332300 | 0.041 | 0.016 | 0.005 | 0.003 | 0.002 | 0.003 | 0.002 | 0.053 | 0.039 |
| **7** | 533000 | 332300 | 0.074 | 0.010 | 0.018 | 0.003 | 0.007 | 0.001 | 0.000 | 0.027 | 0.116 |
| **8** | 533200 | 332300 | 0.074 | 0.020 | 0.018 | 0.018 | 0.007 | 0.007 | 0.003 | 0.027 | 0.090 |
| **9** | 533300 | 332300 | 0.074 | 0.026 | 0.014 | 0.018 | 0.006 | 0.003 | 0.003 | 0.027 | 0.077 |
| **10** | 533900 | 332300 | 0.041 | 0.016 | 0.005 | 0.003 | 0.004 | 0.001 | 0.000 | 0.044 | 0.090 |
| **11** | 533300 | 332400 | 0.074 | 0.023 | 0.014 | 0.018 | 0.006 | 0.008 | 0.002 | 0.035 | 0.64 |
| **12** | 533400 | 332400 | 0.074 | 0.023 | 0.005 | 0.006 | 0.011 | 0.003 | 0.003 | 0.027 | 0.077 |
| **13** | 533500 | 332400 | 0.008 | 0.016 | 0.014 | 0.003 | 0.017 | 0.003 | 0.002 | 0.018 | 0.039 |
| **14** | 533630 | 332400 | 0.008 | 0.016 | 0.009 | 0.015 | 0.011 | 0.001 | 0.002 | 0.018 | 0.039 |
| **15** | 533700 | 332400 | 0.008 | 0.010 | 0.005 | 0.015 | 0.006 | 0.001 | 0.002 | 0.018 | 0.013 |
| **16** | 534000 | 332400 | 0.016 | 0.016 | 0.009 | 0.003 | 0.004 | 0.002 | 0.001 | 0.035 | 0.064 |
| **17** | 534300 | 332400 | 0.008 | 0.016 | 0.005 | 0.003 | 0.002 | 0.002 | 0.002 | 0.027 | 0.013 |
| **18** | 533200 | 332500 | 0.074 | 0.023 | 0.009 | 0.009 | 0.006 | 0.008 | 0.003 | 0.035 | 0.077 |
| **19** | 533630 | 332500 | 0.008 | 0.010 | 0.005 | 0.003 | 0.004 | 0.001 | 0.001 | 0.009 | 0.039 |
| **20** | 534700 | 332500 | 0.008 | 0.026 | 0.005 | 0.003 | 0.002 | 0.001 | 0.001 | 0.009 | 0.052 |
| **21** | 534900 | 332500 | 0.074 | 0.023 | 0.005 | 0.003 | 0.006 | 0.002 | 0.002 | 0.009 | 0.090 |
| **22** | 533200 | 332600 | 0.008 | 0.016 | 0.032 | 0.003 | 0.004 | 0.003 | 0.002 | 0.009 | 0.039 |
| **23** | 535800 | 332700 | 0.008 | 0.007 | 0.005 | 0.003 | 0.002 | 0.001 | 0.000 | 0.009 | 0.039 |
| **24** | 535900 | 332700 | 0.074 | 0.007 | 0.005 | 0.003 | 0.002 | 0.001 | 0.000 | 0.018 | 0.039 |

**Table 6.** PIS and NIS in ACT and AAT

| **Sub-criteria** | **ACT** | | **AAT** | |
|---|---|---|---|---|
| | **PIS** | **NIS** | **PIS** | **NIS** |
| **Rock** | 0.074 | 0.008 | 0.280 | 0.031 |
| **Fault** | 0.026 | 0.007 | 0.296 | 0.074 |
| **Argillic** | 0.032 | 0.005 | 0.446 | 0.064 |
| **Phyllic** | 0.018 | 0.003 | 0.409 | 0.068 |
| **Fe-oxides** | 0.017 | 0.002 | 0.507 | 0.056 |
| **Silicic** | 0.008 | 0.001 | 0.473 | 0.053 |
| **Propylitic** | 0.003 | 0 | 0.320 | 0.036 |
| **Analytical signal** | 0.053 | 0.009 | 0.374 | 0.062 |
| **Cu** | 0.116 | 0.013 | 0.347 | 0.039 |

*AHP-Adjusted-TOPSIS (AAT)*

Steps of the AAT include the following stages:

1-3) These stages in AAT are similar to the steps of the ACT method.
4) Determine PIS and NIS by Eqs. (14-15) based on the normalized decision matrix ($r_{ij}$) in Table 6.
5-6) Compute the weighted Euclidian distances by Eqs. (16-17) and calculate the relative closeness of the alternatives to the ideal solution by Eq. (18).
7) The MPM data values of $M_i^A$ are determined by Eq. (19) as Table 8.

*AHP-Modified-TOPSIS (AMT)*

The procedure of AMT is:
1-5) These stages are repeated as ACT.
6-7) Specify the ideal reference point S, $S^l = 0.031, S^N = 0.133$, and Euclidian distance by Eqs. (20-21) for every sub-criteria, respectively.
8) Compute the normalized MPM values of $M_i^M$ by Eq. (22; Table 8).

*Design concept priority ranking by AHP-SAW (ASAW)*

Comparison matrix and weighted of sub-criteria in SAW are similar to AHP:
1) Determine normalized values by Eq. (23; Table 7).
2) Final rank of attributes in Table 8 is obtained by Eq. (25).

**Table 7.** Normalized values in SAW

| Alternatives | | | Sub-criteria | | | | | | | | |
|---|---|---|---|---|---|---|---|---|---|---|---|
| **Num** | **x(m)** | **y(m)** | **Rock** | **Fault** | **Arg.** | **Phy.** | **Feo.** | **Si.** | **Pro.** | **As.** | **Cu** |
| **1** | 535800 | 331400 | 0.111 | 0.750 | 0.143 | 0.167 | 0.111 | 0.111 | 0.556 | 0.167 | 0.111 |
| **2** | 533500 | 332000 | 1.000 | 0.625 | 1.000 | 0.333 | 0.111 | 0.111 | 0.667 | 0.833 | 0.778 |
| **3** | 533830 | 332200 | 1.000 | 0.625 | 0.143 | 0.167 | 0.111 | 0.111 | 0.444 | 0.833 | 0.778 |
| **4** | 533100 | 332300 | 1.000 | 0.625 | 0.571 | 0.167 | 0.667 | 0.222 | 0.444 | 0.667 | 1.000 |
| **5** | 533600 | 332300 | 1.000 | 0.875 | 1.000 | 0.833 | 0.556 | 0.667 | 0.889 | 0.667 | 0.444 |
| **6** | 534100 | 332300 | 0.111 | 0.625 | 0.143 | 0.167 | 0.111 | 0.333 | 0.556 | 1.000 | 0.333 |
| **7** | 533000 | 332300 | 1.000 | 0.375 | 0.571 | 0.167 | 0.444 | 0.111 | 0.111 | 0.500 | 1.000 |
| **8** | 533200 | 332300 | 1.000 | 0.750 | 0.571 | 1.000 | 0.444 | 0.889 | 1.000 | 0.500 | 0.778 |
| **9** | 533300 | 332300 | 1.000 | 1.000 | 0.429 | 1.000 | 0.333 | 0.444 | 0.889 | 0.500 | 0.667 |
| **10** | 533900 | 332300 | 0.111 | 0.625 | 0.143 | 0.167 | 0.111 | 0.111 | 0.222 | 0.667 | 0.667 |
| **11** | 533300 | 332400 | 1.000 | 0.875 | 0.429 | 1.000 | 0.333 | 1.000 | 0.778 | 0.500 | 0.333 |
| **12** | 533400 | 332400 | 1.000 | 0.875 | 0.143 | 0.167 | 0.667 | 0.333 | 0.889 | 0.333 | 0.333 |
| **13** | 533500 | 332400 | 0.111 | 0.625 | 0.429 | 0.167 | 1.000 | 0.444 | 0.667 | 0.333 | 0.333 |
| **14** | 533630 | 332400 | 0.111 | 0.625 | 0.286 | 0.833 | 0.667 | 0.111 | 0.556 | 0.333 | 0.333 |
| **15** | 533700 | 332400 | 0.111 | 0.375 | 0.143 | 0.833 | 0.333 | 0.111 | 0.667 | 0.333 | 0.111 |
| **16** | 534000 | 332400 | 0.111 | 0.625 | 0.143 | 0.167 | 0.111 | 0.111 | 0.111 | 0.500 | 0.556 |
| **17** | 534300 | 332400 | 0.111 | 0.625 | 0.143 | 0.167 | 0.111 | 0.222 | 0.556 | 0.500 | 0.111 |
| **18** | 533200 | 332500 | 1.000 | 0.875 | 0.143 | 0.333 | 0.222 | 0.889 | 1.000 | 0.167 | 0.556 |
| **19** | 533630 | 332500 | 0.111 | 0.375 | 0.143 | 0.167 | 0.222 | 0.111 | 0.222 | 0.167 | 0.333 |
| **20** | 534700 | 332500 | 0.111 | 1.000 | 0.143 | 0.167 | 0.111 | 0.111 | 0.444 | 0.167 | 0.444 |
| **21** | 534900 | 332500 | 0.074 | 0.023 | 0.005 | 0.003 | 0.006 | 0.002 | 0.002 | 0.009 | 0.090 |
| **22** | 533200 | 332600 | 0.008 | 0.016 | 0.032 | 0.003 | 0.004 | 0.003 | 0.002 | 0.009 | 0.039 |
| **23** | 535800 | 332700 | 0.008 | 0.007 | 0.005 | 0.003 | 0.002 | 0.001 | 0.000 | 0.009 | 0.039 |
| **24** | 535900 | 332700 | 0.074 | 0.007 | 0.005 | 0.003 | 0.002 | 0.001 | 0.000 | 0.018 | 0.039 |

**Table 8.** Illustrative example of applying AHP-TOPSIS and AHP-SAW methods in MPM for 11 criteria as evidential layers and 20 alternatives

| Alternative | | | Sub criteria | | | | | | | | | AHP-TOPSIS | | | AHP-SAW |
|---|---|---|---|---|---|---|---|---|---|---|---|---|---|---|---|
| Num | x(m) | y(m) | Rock | Fault | Arg. | Phy. | Feo. | Si. | Pro. | As. | Cu | ACT | AAT | AMT | ASAW |
| 1 | 535800 | 331400 | 0.031 | 0.222 | 0.064 | 0.068 | 0.056 | 0.053 | 0.178 | 0.062 | 0.039 | 0.000 | 0 | 0.000 | 0.185 |
| 2 | 533500 | 332000 | 0.280 | 0.185 | 0.446 | 0.136 | 0.056 | 0.053 | 0.213 | 0.311 | 0.270 | 0.930 | 0.955 | 0.894 | 0.794 |
| 3 | 533830 | 332200 | 0.280 | 0.185 | 0.064 | 0.068 | 0.056 | 0.053 | 0.142 | 0.311 | 0.270 | 0.853 | 0.860 | 0.845 | 0.724 |
| 4 | 533100 | 332300 | 0.280 | 0.185 | 0.255 | 0.068 | 0.338 | 0.105 | 0.142 | 0.249 | 0.347 | 1.000 | 0.947 | 1.000 | 0.825 |
| 5 | 533600 | 332300 | 0.280 | 0.259 | 0.446 | 0.341 | 0.282 | 0.315 | 0.284 | 0.249 | 0.193 | 0.753 | 0.999 | 0.643 | 0.730 |
| 6 | 534100 | 332300 | 0.155 | 0.185 | 0.064 | 0.068 | 0.056 | 0.158 | 0.178 | 0.374 | 0.116 | 0.436 | 0.776 | 0.319 | 0.370 |
| 7 | 533000 | 332300 | 0.280 | 0.111 | 0.255 | 0.068 | 0.225 | 0.053 | 0.036 | 0.187 | 0.347 | 0.934 | 0.906 | 0.938 | 0.767 |
| 8 | 533200 | 332300 | 0.280 | 0.222 | 0.255 | 0.409 | 0.225 | 0.420 | 0.320 | 0.187 | 0.270 | 0.879 | 0.996 | 0.844 | 0.784 |
| 9 | 533300 | 332300 | 0.280 | 0.296 | 0.191 | 0.409 | 0.169 | 0.210 | 0.284 | 0.187 | 0.231 | 0.784 | 0.932 | 0.758 | 0.747 |
| 10 | 533900 | 332300 | 0.155 | 0.185 | 0.064 | 0.068 | 0.113 | 0.053 | 0.036 | 0.311 | 0.270 | 0.741 | 0.842 | 0.498 | 0.427 |
| 11 | 533300 | 332400 | 0.280 | 0.259 | 0.191 | 0.409 | 0.169 | 0.473 | 0.249 | 0.249 | 0.193 | 0.722 | 0.936 | 0.513 | 0.633 |
| 12 | 533400 | 332400 | 0.280 | 0.259 | 0.064 | 0.136 | 0.338 | 0.210 | 0.320 | 0.187 | 0.231 | 0.752 | 0.884 | 0.467 | 0.553 |
| 13 | 533500 | 332400 | 0.031 | 0.185 | 0.191 | 0.068 | 0.507 | 0.210 | 0.213 | 0.125 | 0.116 | 0.203 | 0.744 | 0.209 | 0.328 |
| 14 | 533630 | 332400 | 0.031 | 0.185 | 0.128 | 0.341 | 0.338 | 0.053 | 0.178 | 0.125 | 0.116 | 0.197 | 0.742 | 0.205 | 0.330 |
| 15 | 533700 | 332400 | 0.031 | 0.111 | 0.064 | 0.341 | 0.169 | 0.053 | 0.213 | 0.125 | 0.039 | 0.027 | 0.683 | 0.030 | 0.214 |
| 16 | 534000 | 332400 | 0.062 | 0.185 | 0.128 | 0.068 | 0.113 | 0.105 | 0.107 | 0.249 | 0.193 | 0.448 | 0.789 | 0.386 | 0.365 |
| 17 | 534300 | 332400 | 0.031 | 0.185 | 0.064 | 0.068 | 0.056 | 0.105 | 0.178 | 0.187 | 0.039 | 0.064 | 0.678 | 0.061 | 0.223 |
| 18 | 533200 | 332500 | 0.280 | 0.259 | 0.128 | 0.205 | 0.169 | 0.473 | 0.320 | 0.249 | 0.231 | 0.793 | 0.922 | 0.593 | 0.606 |
| 19 | 533630 | 332500 | 0.031 | 0.111 | 0.064 | 0.068 | 0.113 | 0.053 | 0.071 | 0.062 | 0.116 | 0.130 | 0.687 | 0.144 | 0.226 |
| 20 | 534700 | 332500 | 0.031 | 0.296 | 0.064 | 0.068 | 0.056 | 0.053 | 0.142 | 0.062 | 0.154 | 0.275 | 0.702 | 0.265 | 0.317 |
| 21 | 534900 | 332500 | 0.280 | 0.259 | 0.064 | 0.068 | 0.169 | 0.105 | 0.249 | 0.062 | 0.270 | 0.747 | 0.816 | 0.737 | 0.663 |
| 22 | 533200 | 332600 | 0.031 | 0.185 | 0.446 | 0.068 | 0.113 | 0.210 | 0.249 | 0.062 | 0.116 | 0.233 | 0.721 | 0.218 | 0.320 |
| 23 | 535800 | 332700 | 0.031 | 0.074 | 0.064 | 0.068 | 0.056 | 0.053 | 0.036 | 0.062 | 0.116 | 0.126 | 0.678 | 0.140 | 0.210 |
| 24 | 535900 | 332700 | 0.280 | 0.074 | 0.064 | 0.068 | 0.056 | 0.053 | 0.036 | 0.125 | 0.116 | 0.474 | 0.756 | 0.421 | 0.444 |

## Results and Discussion

The geochemical, geological, structural, geophysical, and remote sensing are the datasets. These datasets include the 678 stream sediment samples for Cu concentration by the final weight of 0.334 in AHP (Table 2 & Fig. 5).

Anarak 1.00.000 geological map involves lithology and faults which are appropriate parameters to affect the hydrothermal copper deposits especially manto and vein types. The Anarak region consists of intrusive and subvolcanic rocks within Tertiary sediments (Salehi et al., 2020). The alteration index minerals are carbonate, quartz, iron oxides, chlorite, sericite, chalcedony, and albite (Bagheri et al., 2007). Lithology was classified as andesite, muscovite, carbonate, and chlorite-schists forms by the owed final weighting of the AHP method is 0.263 (Table 2 & Fig. 5).

Trends of faults are NE-SW and NW-SE in this region. The major part of the fault density is situated in the northern and NW parts of this district (Fig. 5). The weight of the fault's sub-criteria is 0.088 which is revealed in Table 2. The airborne magnetic geophysical data is useful for the ores' exploration. The final weight of this layer is estimated as 0.142 (Table 2). Main anomalies occurred in the NW, north, and south of this region (Fig. 5).

A fundamental step for hydrothermal ore deposits exploration is the alteration zone's detection based on remote sensing data (Fakhari et al., 2019; Novruzov et al., 2019; Mirsepahvand et al., 2022; Saed et al., 2022). There are phyllic, argillic, silicification, iron oxides, and propylitic alterations zone by Aster and ETM data. The final weights for each alteration zone were evaluated by AHP as depicted in Table 2 and Fig. 4. The argillic alteration is expanded with an NNW trend. Its first and highest weight is 0.071 in this region. The phyllic and iron oxides have second and third ranks which are 0.045, 0.033 (Table 2). Silicification and propylitic alteration zones have the fourth and fifth ranks by the low weights that equal to 0.016 and 0.010, and also; they occurred in the north, NW, and SE parts.

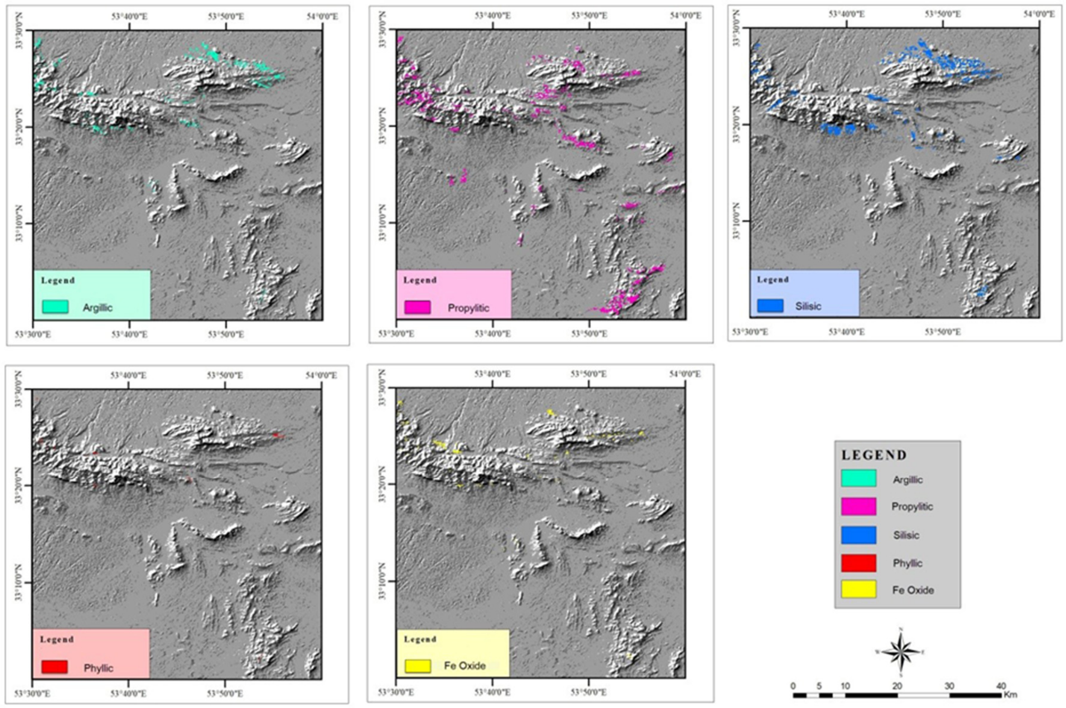


**Figure 4.** Remote sensing layers extracting alteration zones from the ASTER data

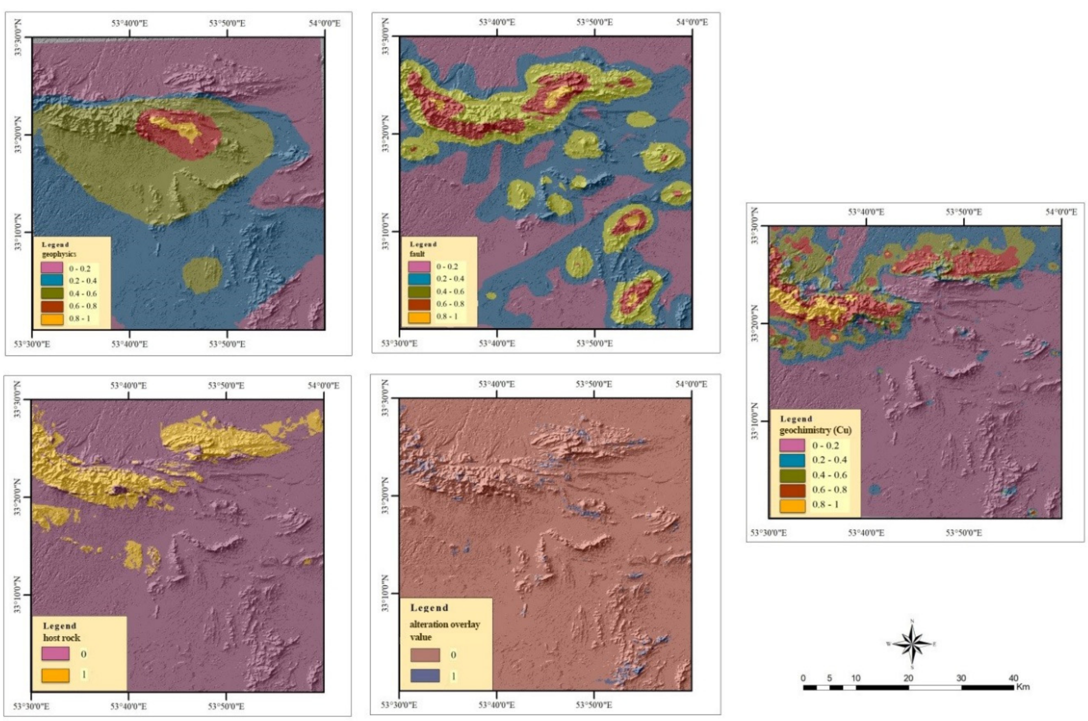


**Figure 5.** The dataset for alteration overlay with density of fault, geophysics, host rock, and geochemistry were transformed to the interval of [0,1]

Finally, AHP-weights used in Eqs. (5), (7), (16), and (17) of different TOPSIS and Eq. (25) of SAW (Table 8). MPMs are illustrated for the ACT, AAT, AMT and ASAW in Figures 6 and 7. Results of these methods represent that major copper prospects exist in the north part of this region especially in the NW part of the Anarak region. The known Cu deposits/mineralization specifically manto type are overlapped with these prospects, as depicted in Figs 6-7. Consequently, results derived via these methods were overlapped as couple positions (Fig. 8).

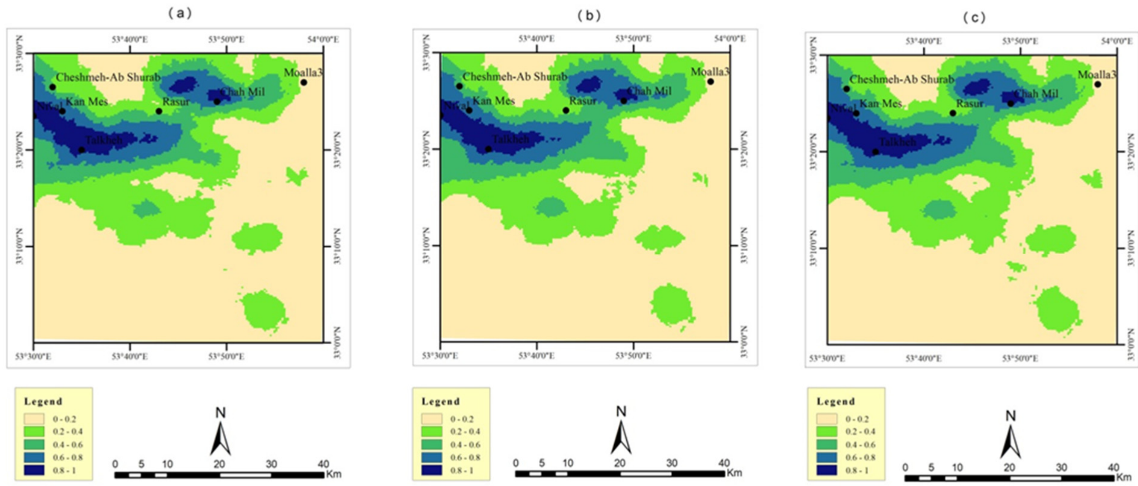


**Figure 6.** The plot of AHP-TOPSIS MPMs, (a) the AHP-Adjusted-TOPSIS (AAT), (b) AHP-Modufied-TOPSIS (AMT) and (c) AHP-Conventional-TOPSIS (ACT), on all maps the location of active copper mines has been superimposed

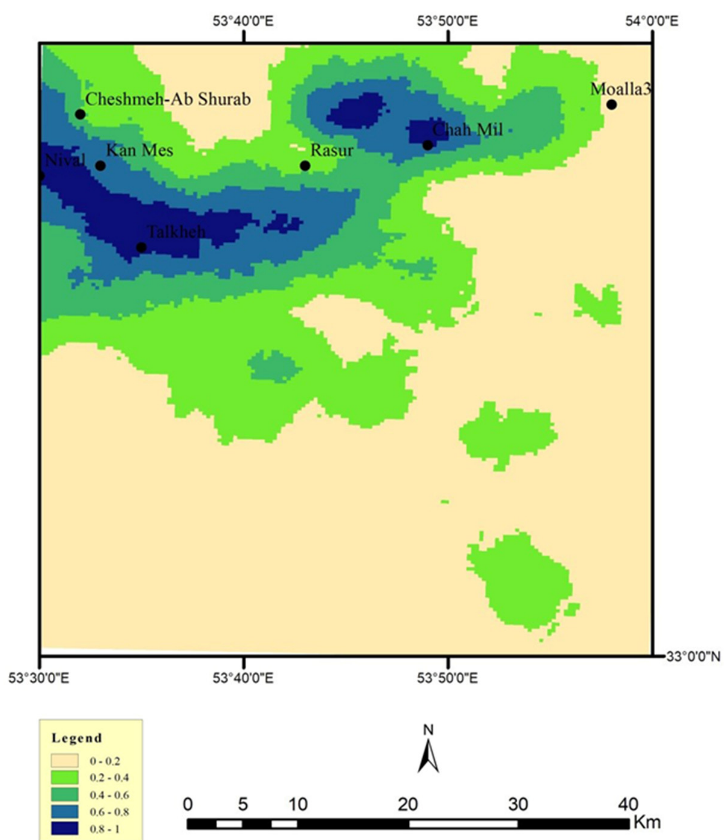


**Figure 7.** The plot of AHP-SAW (ASAW) MPM and the locations of active copper mines/deposits

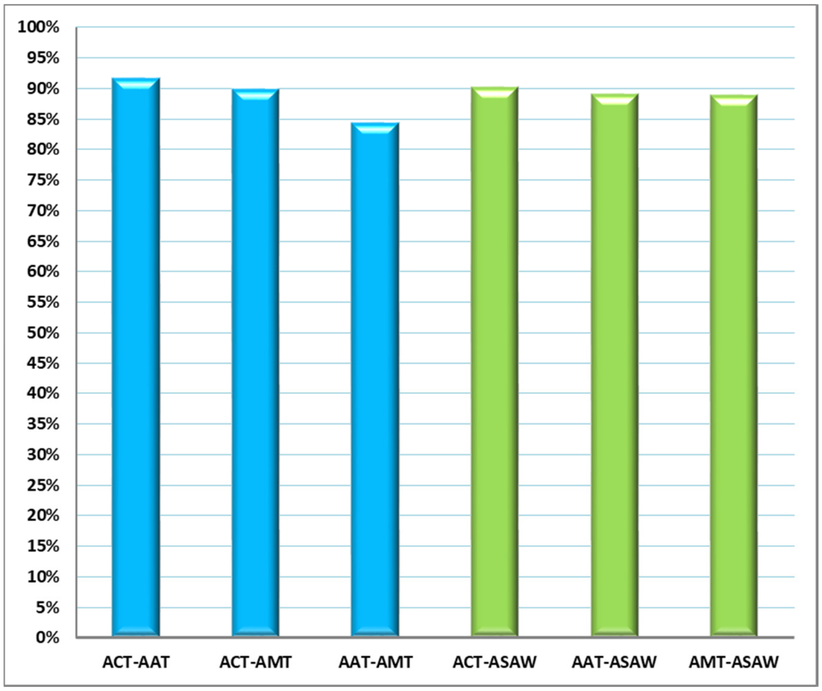


**Figure 8.** The chart of percent overlap of couple methods with together, ACT-AAT (91.80%), ACT-AMT (89.98%), AAT-AMT (84.53%), ACT-ASAW (90.27%), AAT-ASAW (89.24%), and AMT-ASAW (88.95%).

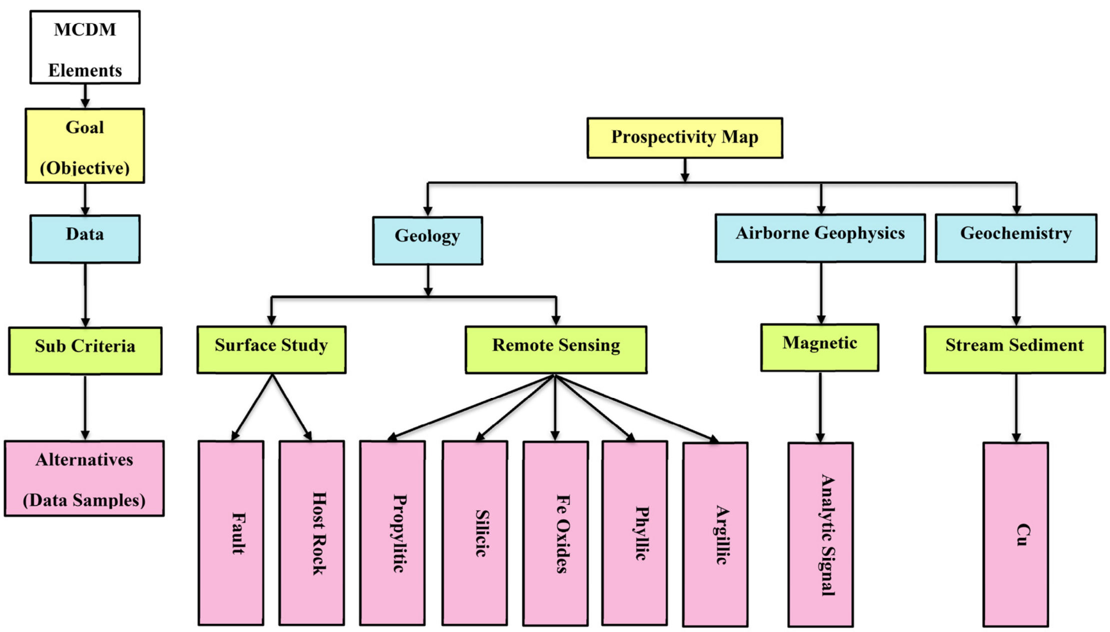


**Graphical Abstract**

The couple methods can divide two parts, couples of TOPSIS-TOPSIS and TOSIS-SAW methods (Fig. 8). The Highest overlapping value equals 91.80% for ACT-AAT.

## Conclusion

The AHP-TOPSIS and AHP-SAW methods were utilized with the appropriate solutions for finding the copper prospects by GIS and overcome difficulties of the Anarak region which has a high potential of metallic deposits in Central Iran. Main copper prospects identified in the NW and northern parts of the study region. In addition, the correlation between the location of known copper mineralization and main prospects can be present copper manto type ores in this region. On the other hand, appropriate correlation with copper mines and main copper deposits/occurrences in the Anarak region.

The couple methods can divide two parts, couples of TOPSIS-TOPSIS and TOSIS-SAW methods. The highest percent overlap belongs to the TOPSIS-TOPSIS method, ACT-AAT by a percent of 91.80%. The couple of ACT-ASAW in TOPSIS-SAW method has the second rank of 90.27% but the validity of the ACT-ASAW method is higher than the ACT-AAT method because two different methods have been used. In this study, three methods of TOPSIS were carried out based on weighting by AHP method. Main advantage of this methodology is using of simultaneously the TOPSIS and SAW methods with AHP weighting and matrix operator with determination solving approaches according to positive and negative parameters. Combination of these methods can be provided appropriate answer for generation of the MPM.

## References

Abedi, M., Norouzi, G., 2016. A general framework of TOPSIS method for integration of airborne geophysics, satellite imagery, geochemical and geological data. International Journal of Applied Earth Observation and Geoinformation, 46: 31-44.

Bagheri, H., 2015. Crustal lineament control on mineralization in the Anarak area of Central Iran. Ore Geology Reviews, 66: 293-308.

Bagheri, H., Moore, F.D., Alderton, H.M., 2007. Cu-Ni-Co-As (U) mineralization in the Anarak area of central Iran. Journal of Asian Earth Sciences, 29: 651-665.

Buchs, D. M., Bagheri, S., Martin, L., Hermann, J., Arculus, R., 2013. Paleozoic to Triassic ocean opening and closure preserved in Central Iran: Constraints from the geochemistry of meta-igneous rocks of the Anarak area: Lithos, 172-173, 267-287.

Chen, S.J., Hwang, C.L., 1992. Fuzzy Multiple Attribute Decision Making: Method sand Applications. Springer-Verlag, Berlin.

Churchman, C.W., Ackoff, R.L., 1954. An approximate measure of value. J. Oper. Res. Soc. Am, 2(2): 172-187.

Deng, H., Yeh, C. H., Willis, R.J., 2000. Inter-company comparison using modified TOPSIS with objective weights. Comput. Oper. Res, 27: 963-973.

Fakhari, S., Jafarirad, A., Afzal, P., Lotfi, M., 2019. Delineation of hydrothermal alteration Zones for porphyry systems utilizing ASTER data in Jebal barez area, SE Iran. Iranian Journal of Earth Sciences, 11: 80-92.

Ferrier, G., Ganas, A., Pope, R., 2019. Prospectivity mapping for high sulfidation epithermal porphyry deposits using an integrated compositional and topographic remote sensing dataset. Ore Geology Reviews, 107:353-363.

Ghaeminejad, H., Abedi, M., Afzal, P., Zaynali, F., Yousefi, M., 2020. A fractal-based outranking approach for mineral prospectivity analysis. Bollettino di Geofisica Teorica e Applicata, 61(4): 555-588.

Hwang, C.L., Yoon, K., 1981. Multiple Attributes Decision Making Methods and Applications, Springer, Berlin Heidelberg, Germany.

Jebeli, M., Afzal, P., Pourkermani, M., Jafari Rad, A., 2020. Characteristics of fluid inclusions in the Cenozoic volcanic-hosted Kushk-e-Bahram Manto-type Cu deposit of central Iran. Geologos, 26: 127–137.

Mirsepahvand, F., Jafari, M.R., Afzal, P., Arian, M.A., 2022. Identification of Alteration Zones using ASTER Data for Metallic Mineralization in Ahar region, NW Iran. Journal of Mining and Environment 13(1): 309-324

Novruzov, N., Valiyev, A., Bayramov, A., Mammadov, S., Ibrahimov, J., Ebdulrehimli, A., 2019. Mineral composition and paragenesis of altered and mineralized zones in the Gadir low sulfidation epithermal deposit (Lesser Caucasus, Azerbaijan). Iranian Journal of Earth Sciences, 11: 14-29.

Opricovic, S., Tzeng, G.H., 2004. Compromise solution by MCDM methods: a comparative analysis of VIKOR and TOPSIS. Eur J Oper Res, 156(2): 445-455.

Panahi, S., Khakzad, A., Afzal, P., 2017. Application of Step-wise Weight Assessment Ratio Analysis (SWARA) for copper prospectivity mapping in Anarak region, central Iran. Arabian Journal of Geosciences 10: 484 (2-17).

Rent, L., Zhang, Y., Wang, Y., Sun, Z., 2007. Comparative analysis of a novel MTOPSIS method and TOPSIS. Appl. Math. Res. Express 10, http://dx.doi.org/10.1093/amrx/abm005, Article ID abm005.

Pazand, K., Hezarkhani, A., 2015. Porphyry Cu potential area selection using the combine AHP—TOPSIS methods: a case study in Siahrud area (NW Iran). Earth. Sci. Info, 8: 207-220.

Saaty, T.L., Vargas, L.G., 2001. Models, methods, concepts & applications of the Analytic Hierarchy Process. International Series in Operations Research & Management Science. Springer, Berlin, 34.

Saed, S., Azizi, H., Daneshvar, N., Afzal, P., Whattam, S.A., Mohammad, Y.O., 2022. Hydrothermal alteration mapping using ASTER data, Takab-Baneh area, NW Iran: A key for further exploration of polymetal deposits. Geocarto International, 1-25.

Salehi, M.A., Bahrami, A., Moharrami, S., Vaziri-Moghaddam, H., Pakzad, H.R., Shakeri, B., 2020. Palaeoenvironmental and sequence-stratigraphic analysis of the Middle-Late Devonian carbonates (Bahram Formation) of Anarak, western Central Iran. Journal of African Earth Sciences, 171: 103938.

Tarkian, M., Bock, W. D., Neumann, M., 1983. Geology and mineralogy of the Cu−Ni−Co−U ore deposits at Talmessi and Meeskani, central Iran: Tschermaks mineralogische und petrographische Mitteilungen, 32: 111-133.

Ying, X., Guang-Ming, Z., Gui-Qiu, C., Lin, T., Ke-Lin, W., Dao-You, H., 2007. Combining AHP with GIS insynthetic evaluation of eco-enviroment quality-A case study of Hunan Province, China. Ecol Model, 209: 97-109.

Zavadskas, E.K., Vainiunas, P., Turskis, Z., Tamosaitiene, J., 2012. Multiple criteria decision support system for assessment of projects managers in construction. Int. J. Inf. Technol. Decis. Mak, 11(02): 501-520.

Zhang, N., Zhou, K., Du, X., 2017. Application of fuzzy logic and fuzzy AHP to mineral prospectivity mapping of porphyry and hydrothermal vein copper deposits in the Dananhu-Tousuquan island arc, Xinjiang, NW China. Journal of African Earth Sciences, 128: 84-96.

Zhu, G.N., Hu, J., Ren, H., 2020. A fuzzy rough number-based AHP-TOPSIS for design concept evaluation under uncertain environments. Applied Soft Computing, 91: 106228.